High-spin states in ^{136}Ce: Systematics of collective oblate rotation

E. S. Paul,* D. B. Fossan, Y. Liang, R. Ma, and N. Xu
Department of Physics, State University of New York at Stony Brook, Stony Brook, New York 11794

R. Wadsworth
Department of Physics, University of York, Heslington, York Y01 5DD, United Kingdom

I. Jenkins and P. J. Nolan
Oliver Lodge Laboratory, University of Liverpool, P.O. Box 147, Liverpool L69 3BX, United Kingdom
(Received 11 December 1989)

The level structure of the transitional even-even ^{136}Ce nucleus has been investigated using the ^{122}Sn(^{18}O, $4n\gamma$) reaction. The prominent structure observed at high spin is a $\Delta I=1$ rotational band, populated with $\sim 25\%$ intensity of the $2^+ \rightarrow 0^+$ transition, which has a low dynamic moment of inertia $<20\hbar^2$ MeV^{-1} for frequencies below $\hbar\omega=0.45$ MeV. This band is interpreted in terms of a two-quasiproton-two-quasineutron configuration with a shape close to the collectively rotating $\gamma=-60°$ oblate shape, and is related to the oblate $\pi h_{11/2}\otimes[\nu h_{11/2}]^2$ configuration seen in several nearby odd-Z nuclei. The systematics of such oblate rotational bands in this mass region are discussed. Other $\Delta I=2$ bands, built on states including $h_{11/2}$ quasineutron orbitals, are also associated with collective oblate rotation. In addition, tentative evidence is presented for a weak band ($<2\%$ intensity), showing an enhanced dynamic moment of inertia $\sim 57\hbar^2$ MeV^{-1}, built on the highly deformed $[\nu i_{13/2}]^2$ prolate configuration.

I. INTRODUCTION

The transitional nuclei in the light rare-earth region of mass $A\sim 135$, just below the neutron shell closure at $N=82$, exhibit a variety of interesting phenomena. These nuclei are predicted to be soft[1-3] with respect to γ, the shape asymmetry parameter in the polar representation of rotating quadrupole shapes, and shape changes can readily be achieved by the rotational alignment of specific quasiparticle pairs.[4,5] Whereas valence $h_{11/2}$ protons stabilize near-prolate $\gamma\sim 0°$ shapes (the Lund convention[6] is used for the definition of γ), valence $h_{11/2}$ neutrons can induce significant shape changes towards the collectively rotating oblate $\gamma=-60°$ shape. Strongly coupled $\Delta I=1$ rotational bands, built on multiquasiparticle states with such an oblate shape, have recently been established in odd-Z ^{131}La,[7] ^{133}Pr,[8] and ^{137}Pr;[9] doubly-odd ^{128,130}La;[10] and even-even ^{132}Ba.[11] In this paper, evidence is presented for a similar strongly populated $\Delta I=1$ band in ^{136}Ce, and the systematics of such bands are discussed. The important components of these oblate bands appear to be a high-Ω $h_{11/2}$ proton coupled to a pair of rotationally aligned low-Ω $h_{11/2}$ neutrons at $\gamma\sim -60°$.

An additional interest in the cerium nuclei arises because of the observation of highly deformed $\Delta I=2$ decoupled bands in ^{131,132}Ce (Refs. 12 and 13) with a quadrupole deformation $\beta_2\geq 0.35$ ($\gamma\sim 0°$) corresponding to a prolate rotor with a 3:2 axis ratio. Recent total-Routhian-surface (TRS) cranking calculations[14,15] have also predicted low-lying highly deformed prolate bands in $^{133-136}$Ce associated with one or more $\nu i_{13/2}$ β-driving orbitals. In ^{133}Ce, a decoupled band has been associated with the $\nu i_{13/2}$ orbital,[16] but the observed 25% increase in the moment of inertia, although indicating a larger quadrupole deformation than the ground state, does not suggest a highly deformed ($\beta_2\sim 0.35$) structure. Searches for such a highly deformed band in ^{133}Ce have proven unsuccessful,[17,18] while the analysis of ^{134,135}Ce from the present data is still in progress. However, tentative evidence for a band of enhanced deformation in ^{136}Ce will be presented in this paper.

Low-lying states in ^{136}Ce have previously been discussed by Ward *et al.*,[19] Dehnhardt *et al.*,[20] and Müller-Veggian *et al.*[21] In addition, an isomeric 10^+ state has been established by Yoshikawa[22] and the nature of this isomer has been discussed by Dafni *et al.*[23]

II. EXPERIMENTAL METHODS AND RESULTS

A. Coincidence experiments

The ^{122}Sn(^{18}O, $xn\gamma$)$^{140-x}$Ce reaction at beam energies of 85 and 89 MeV was used to investigate high-spin states of the ^{134,135,136}Ce nuclei. Two stacked self-supporting ^{122}Sn targets of thickness 500 μg/cm^2 were bombarded by beams of ^{18}O accelerated at the Stony Brook Superconducting LINAC Facility such that the majority of the recoiling nuclei left the target material with the full recoil velocity prior to γ-ray emission. An array of six Compton-suppressed Ge detectors[24] was used to record γ-γ coincidence data. In order to improve the resolution of the Doppler shifted transitions, lead tapered-slit collimators were inserted in front of the Ge detectors such that an opening half-angle $\Delta(\theta/2)=4.6°$ was achieved.

The effects on the energy resolution when using thin targets and a small angular acceptance are discussed by Wyss in Ref. 25. Gamma-ray multiplicity information was also recorded by fourteen hexagonal bismuth germanate (BGO) crystals covering a solid angle in excess of 80% of 4π. This Stony Brook array is shown schematically in Fig. 1.

In order to reduce background activity and Coulex lines, only those Ge-Ge events in coincidence with at least two BGO elements were written onto magnetic tape. Under this condition, approximately 120 million two- or higher-order Ge-Ge events were recorded at 85 MeV while 160 million events were recorded at 89 MeV. In order to emphasize the $4n$ channel into ^{136}Ce, only those events with fold k (the number of BGO elements firing) in the range $7 \leq k \leq 14$ for the 85-MeV bombardment were sorted offline on a MICROVAX II computer to produce a symmetrized array of E_γ vs E_γ. Approximately 75 million events were sorted into this array. The background, arising from many weak unresolved continuum γ rays and from Compton scattering of the strong discrete lines, was subtracted channel by channel from this array using the method outlined in Ref. 26. Gated spectra generated from this array were used to construct the decay scheme of ^{136}Ce, which is presented in Fig. 2. Examples of such gated coincidence spectra are shown in Fig. 3.

B. Angular distribution and correlation data

A subsequent angular distribution measurement was undertaken for the transitions in ^{135,136}Ce using the ^{124}Sn(^{16}O, $xn\gamma$)$^{140-x}$Ce reaction. A 91-MeV ^{16}O beam was used to bombard a ^{124}Sn target of thickness 2.3 mg/cm^2 on a natural lead backing of 50 mg/cm^2. One Compton-suppressed Ge detector, 22 cm from the target, was positioned at angles 90°, 115°, 125°, 135°, and 145° with respect to the beam axis. A second Ge detector at −90° served as a monitor. The empirical γ-ray intensities were fitted to the standard Legendre expansion

$$W(\theta) = A_0 + A_2 P_2(\cos\theta) + A_4 P_4(\cos\theta) , \quad (1)$$

where A_0, A_2, and A_4 are adjustable parameters. The results of this analysis are presented in Table I, where a small correction has been made to each A_2/A_0 and A_4/A_0 value to account for the finite size of the detector. For other transitions assigned to ^{136}Ce that were weak or formed doublets in the singles spectra, the intensities were obtained from the coincidence data. These values are also included in Table I. The transition intensities have been corrected for both detector efficiency and internal conversion effects.

An angular correlation analysis was also performed making use of the coincidence data. When recording the coincidence data, the six Ge detectors, 14.2 cm distant from the target, had been placed at angles of ±145°, ±28°, −85°, and +80° with respect to the beam axis. The two detectors nearest 90° (−85° and +80°) were sorted against the other four detectors to produce a two-dimensional angular correlation array, from which it was possible to extract average empirical directional correlation (DCO) (Ref. 27) intensity ratios. Gates were set on known quadrupole transitions along both axes of the correlation array. The intensity ratios of other coincident transitions observed in the two spectra obtained for each gating transition were used to distinguish between dipole and quadrupole transitions. The empirical intensity ratios extracted for stretched quadrupole transitions in this and neighboring nuclei are typically ≥ 1.0, while values ≤ 0.7 are obtained for stretched dipole transitions. The results of this angular correlation analysis, averaged for several gating quadrupole transitions, are included in Table I.

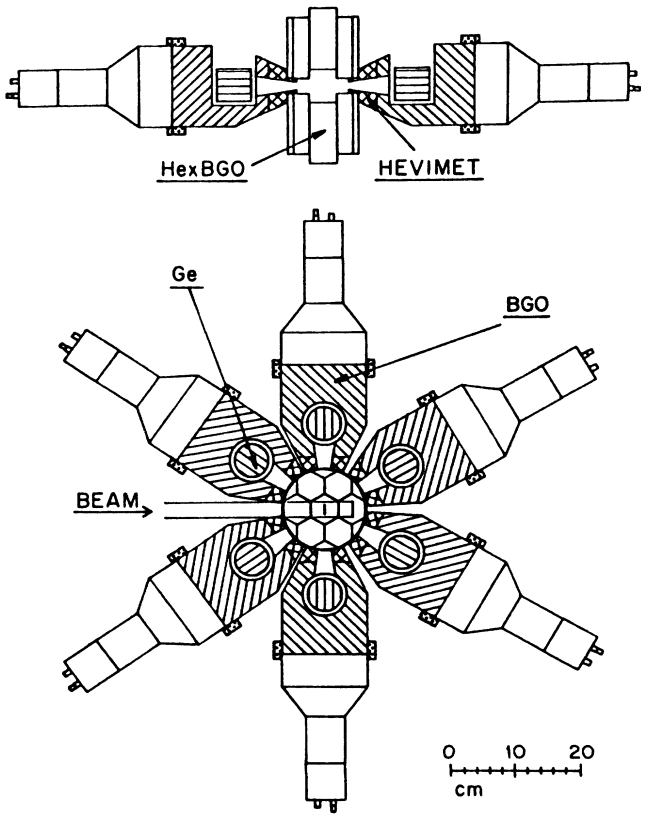

FIG. 1. A schematic view of the SUNY array.

C. The decay scheme of ^{136}Ce

The decay scheme of ^{136}Ce, deduced from this study, is shown in Fig. 2. The placement of the γ transitions in the level scheme is based on coincidence relations and relative intensities. The spin-parity assignments were deduced from the angular distribution and correlation analysis, together with the observed decay patterns.

The somewhat irregular ground-state band could be followed up to $I^\pi = 8^+$. Shown to the right in Fig. 2 is the 10^+ state with a measured half-life $t_{1/2} = 2.2$ μs.[22] The g factor of this state has been measured by Dafni *et al.*[23] as $g \sim -0.18$ indicating a $[\nu h_{11/2}]^2$ configuration for this state. Two quadrupole transitions have been observed above this isomeric level up to the 14^+ level at 4834 keV. Several other transitions, mainly dipole in nature, have been placed above the 4834-keV level. In addition, several low-lying negative-parity states are shown to

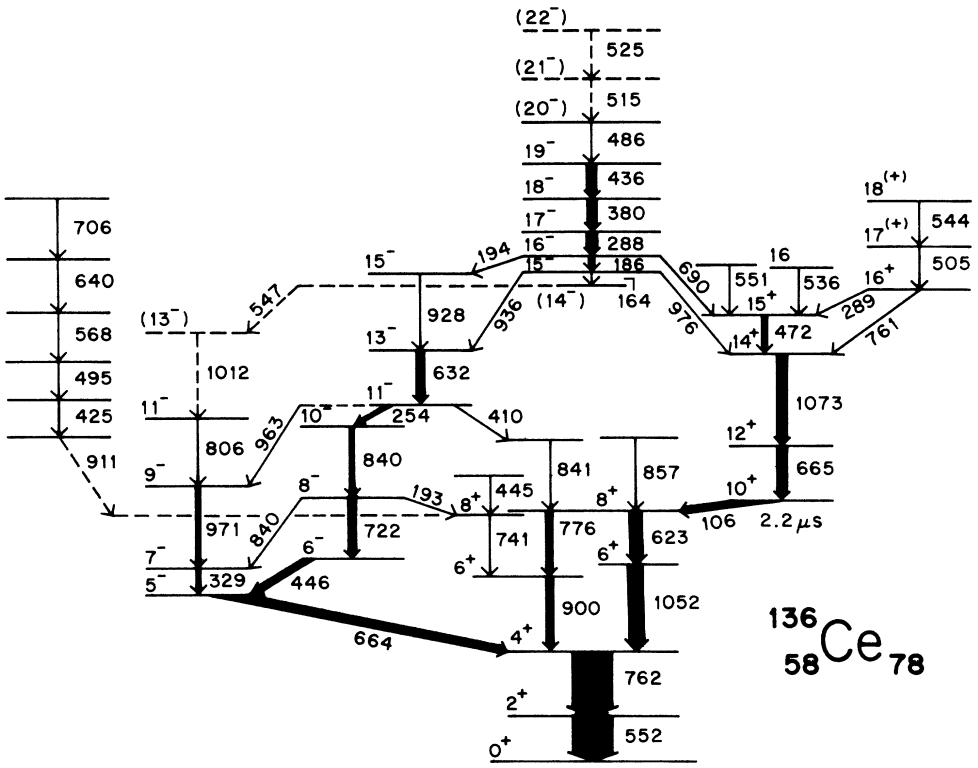

FIG. 2. The decay scheme of ^{136}Ce deduced from this work. The transition energies are given in keV and the width of the arrows represents the relative transition intensities.

the left in Fig. 2 that are connected predominantly by stretched quadrupole transitions.

Shown at the highest spins is a relatively strongly populated $\Delta I=1$ band. A γ-ray spectrum showing transitions within this band is presented in Fig. 3(a). The ordering of the two topmost transitions of energies 515 and 525 keV is not certain and hence they are shown dashed in Fig. 2. This band decays by in-band $\Delta I=1$ transitions with none of the crossover $E2$ transitions being observed despite the intensity of the band. Reliable angular distribution data could only be extracted for the 380 and 436 keV transitions; the values are consistent with negative $E2/M1$ mixing ratios $\delta_{E2/M1}$ (using the sign convention of Ref. 28) for these $\Delta I=1$ transitions (see Table I).

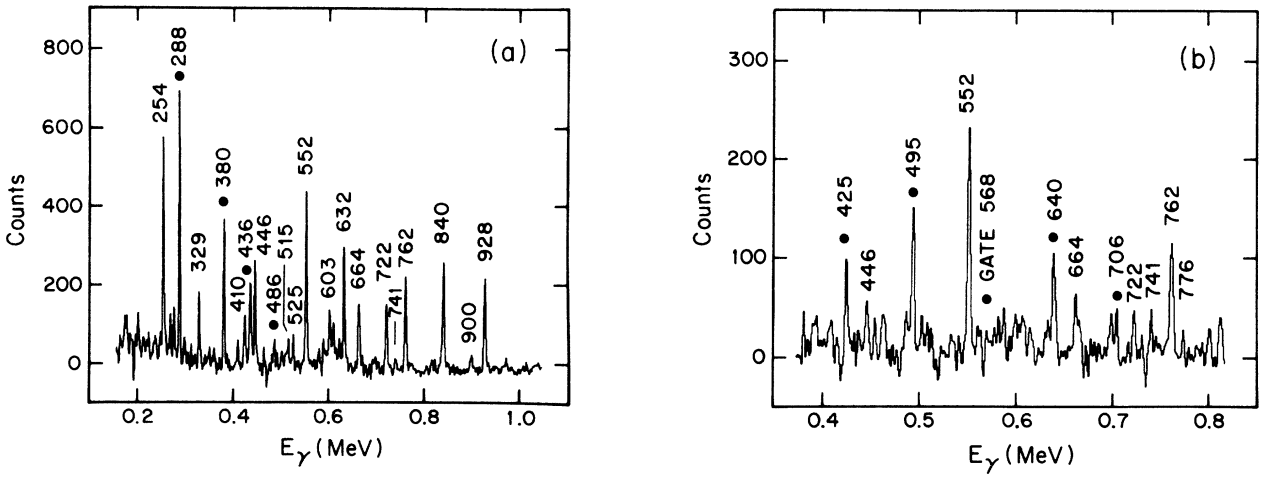

FIG. 3. Examples of gated coincidence spectra with transition energies labeled in keV: (a) A gate set on the 194 keV ($16^- \rightarrow 15^-$) transition depopulating the $\Delta I=1$ band (this transition forms a doublet with the weaker 193 keV $8^- \rightarrow 8^+$ transition). The transitions marked with solid circles are associated with the $\Delta I=1$ band. The rise in the background at low energies is a consequence of the background-subtraction technique (Ref. 26). (b) A gate set on the 568 keV transition showing evidence for a weak band (solid circles) with $\Delta E_\gamma \sim 70$ keV.

TABLE I. Energies, intensities, and angular distribution data for the transitions assigned to ^{136}Ce following the ^{122}Sn(^{18}O,4$n\gamma$) reaction.

E_γ[a] keV	Rel.[b] intensity	A_2/A_0	A_4/A_0	DCO[c] ratio	Multipolarity	Assignment	E_γ[a] keV	Rel.[b] intensity	A_2/A_0	A_4/A_0	DCO[c] ratio	Multipolarity	Assignment
105.6	40(3)	+0.259(47)	+0.037(53)		$E2$	$10^+\rightarrow 8^+$	550.7	<2					$\rightarrow 15^+$
158	<2						552.1	≡100	+0.264(38)	−0.019(42)		$E2$	$2^+\rightarrow 0^+$
164	<2					$15^-\rightarrow(14^-)$	568	<2					
169	<2						623.3	31(1)	+0.328(44)	+0.068(51)		$E2$	$8^+\rightarrow 6^+$
186.0	12(1)	−0.155(43)	≡0.0	0.78(4)	($M1/E2$)	$16^-\rightarrow 15^-$	632.1	25(3)	e	e	1.3(1)	$E2$	$13^-\rightarrow 11^-$
189	<2						640	<2					
193	<2			0.7(1)		$8^-\rightarrow$	664.3	35(3)	f	f	0.86(4)	$E1$	$5^-\rightarrow 4^+$
194.0	4(1)				($M1/E2$)	$(16^-\rightarrow 15^-)$	665.2	35(3)			0.9(1)	$E2$	$12^+\rightarrow 10^+$
201	<2						689.7	6(1)			0.6(1)	$E1$	$16^-\rightarrow 15^+$
234	<2						706	<2					
253.7	12(2)	−0.211(47)	+0.008(59)	0.58(4)	$M1/E2$[d]	$11^-\rightarrow 10^-$	721.8	20(3)	e	e	1.2(1)	$E2$	$8^-\rightarrow 6^-$
288.1	25(2)	−0.184(40)	−0.004(51)	0.69(4)	$M1/E2$	$17^-\rightarrow 16^-$	741	4(1)	+0.23(12)	+0.13(14)	0.9(2)	$E2$	$8^+\rightarrow 6^+$
288.9					$M1/E2$	$16^+\rightarrow 15^+$	761.0	13(4)	+0.335(38)	−0.031(42)	1.0(1)	$E2$	$16^+\rightarrow 14^+$
293	<2						762.3	100(5)			1.05(4)	$E2$	$4^+\rightarrow 2^+$
328.8	13(1)	+0.356(54)	−0.059(62)	1.4(1)	$E2$	$7^-\rightarrow 5^-$	775.8	21(1)	+0.319(50)	+0.084(57)	1.2(2)	$E2$	$8^+\rightarrow 6^+$
379.9	30(2)	−0.345(36)	−0.034(47)	0.69(5)	$M1/E2$	$18^-\rightarrow 17^-$	806.2				1.0(1)	$E2$	$11^-\rightarrow 9^-$
384	<2						839.5					$M1/E2$[d]	$8^-\rightarrow 7^-$
410	<2					$11^-\rightarrow$	840.3	25(2)				$E2$[d]	$10^-\rightarrow 8^-$
425	<2						841						$\rightarrow 8^+$
445	<2						857	<2					$\rightarrow 8^+$
436.5	23(3)	−0.453(44)	−0.006(57)	0.72(6)	$M1/E2$	$19^-\rightarrow 18^-$	899.9	25(1)	+0.277(43)	−0.052(49)	1.2(1)	$E2$	$6^+\rightarrow 4^+$
445	<2					$\rightarrow 8^+$	911	<2					
446.4	22(1)	−0.503(44)	−0.112(57)	0.59(4)	$M1/E2$	$6^-\rightarrow 5^-$	928.0		e	e	1.3(2)	$E2$	$15^-\rightarrow 13^-$
471.9	18(2)	−0.305(48)	−0.025(60)	0.40(3)	$M1/E2$	$15^+\rightarrow 14^+$	936.1	7(1)	+0.51(10)	−0.04(10)	1.0(1)	$E2$	$15^-\rightarrow 13^-$
486.5	5(1)					$(20^-)\rightarrow 19^-$	962.5	<2					$11^-\rightarrow 9^-$
495	<2						970.9	9(1)	+0.376(79)	+0.023(91)	1.3(1)	$E2$	$9^-\rightarrow 7^-$
504.8	10(2)			0.5(1)	($M1/E2$)	$17^{(+)}\rightarrow 16^+$	976	<2			0.7(1)	$E1$	$15^-\rightarrow 14^+$
515	<2					$(21^-\rightarrow 20^-)$	1012	<2					$(13^-)\rightarrow 11^-$
525	<2					$(22^-\rightarrow 21^-)$	1052.4	40(1)	+0.276(41)	−0.032(46)		$E2$	$6^+\rightarrow 4^+$
547	<2					$(14^-\rightarrow 13^-)$	1072.7	33(1)	+0.465(46)	−0.061(49)		$E2$	$14^+\rightarrow 12^+$
536.0	4(1)			0.5(1)	($M1/E2$)	$16^{(+)}\rightarrow 15^+$							
543.7	4(1)			0.4(1)	($M1/E2$)	$18^{(+)}\rightarrow 17^{(+)}$							

[a]Transition energies are accurate to ±0.3 keV except those values quoted as integers that are accurate to ±1 keV.
[b]The transtion intensties were obtained mainly from the angular distribution data.
[c]Angular correlation ratios are average values obtained from several gating quadrupole transitions.
[d]Adopted from Ref. 21.
[e]Doublet with a transition in a neighboring nucleus.
[f]Angular distributions for the 664.3/665.2 keV doublet have been extracted in Ref. 21 consistent with these assignments.

Finally, two weak sets of coincident transitions were established with intensities less then 2% of the $2^+ \rightarrow 0^+$ transition. One set of transitions is shown to the extreme left in Fig. 2. These γ rays are in coincidence with the low-lying 552-762-900-741 keV sequence. In addition, all of these transitions are coincident with a 911 keV transition. This 911 keV transition may therefore form the link, or part of the link, between the two bands, but because of the uncertainty, it is shown dashed in Fig. 2. It is assumed that the new transitions are of stretched quadrupole character because of the regular nature of the transitions observed to high transition energies. A constant energy spacing $\Delta E_\gamma \sim 70$ keV is observed in this band. A gate set on the 568 keV transition is presented in Fig. 3(b) showing the weak band.

The second weak set of transitions of energies 189-158-201-169-384-234-293 keV (not included in Fig. 2) that probably feeds the (right-hand) 8^+ level at 2990 keV via the 857 keV and other transitions was established. Some of the higher γ rays in this sequence are also in coincidence with the 665–1073 keV transitions above the isomeric 10^+ level. The ordering of the transitions is taken from individual gated spectra. Because of the low energies of the transitions, they are most likely of $\Delta I = 1$ character.

III. DISCUSSION

A. The ground-state band

The low-lying 552-762-900 keV sequence was initially established by Ward *et al.*[19] who interpreted these transitions as members of the ground-state rotational band of ^{136}Ce up to the first $I^\pi = 6^+$ level at 2214 keV. A second 6^+ level occurs at a higher excitation energy of 2367 keV. By applying the variable moment of inertia (VMI) model,[29] Müller-Veggian *et al.*[21] suggested that this second 6^+ state and the higher 8^+ state at 2990 keV are not collective and proposed $[\pi g_{7/2}]^2$ (6^+) and $[\nu h_{11/2}]^2$ (8^+) configurations, respectively. In addition, the measured $B(E2;4^+ \rightarrow 2^+)$ value of ~ 8 W.u. (Ref. 20) indicates a low collectivity for the ground-state band. Moreover, the ground states of the $76 \leq N \leq 80$ even-even nuclei of this mass region are predicted to exhibit small quadrupole deformations together with significant triaxial deformations,[3,14] while stable prolate deformations $\beta_2 \geq 0.2$ occur for $N \leq 74$. Indeed, recent TRS cranking calculations[14] for ^{136}Ce predict a shallow minimum at $(\beta_2 = 0.06, \gamma = +13°)$ for the ground-state rotational band.

B. The sidebands

1. Positive-parity states

The g-factor measurement of Dafni *et al.*[23] has implied a $[\nu h_{11/2}]^2$ configuration for the isomeric 10^+ level in ^{136}Ce. Because of the shape-driving forces[4,5] that are applied to the γ-soft core by the aligned $h_{11/2}$ neutrons, it is expected that this 10^+ state possesses a shape close to the collectively rotating $\gamma = -60°$ oblate shape. Similar oblate shapes have been proposed in several $N=76$ (Refs. 11, 30, and 31) and $N=78$ (Ref. 32) isotones, while recent TRS calculations for such a configuration in ^{128}Ba are presented in Ref. 33.

Above the 14^+ state at 4834 keV, several other positive-parity states, connected by relatively high-energy $\Delta I = 1$ transitions, have been established. The structure of these states is not clear and will not be discussed further.

2. Negative-parity states

Following comparisons with isomeric states observed in neighboring odd-N nuclei, Müller-Veggian *et al.*[21] proposed a $\nu h_{11/2} \otimes \nu s_{1/2}(d_{3/2})$ configuration (the $\nu s_{1/2}$ and $\nu d_{3/2}$ orbitals are strongly mixed) for the low-lying 5^-, 6^-, 7^- . . . states in ^{136}Ce, with possibly a large negative γ deformation $\gamma \ll 0°$. Specifically, $\frac{19}{2}^+$ isomers have been observed in several $N=77$ isotones including ^{135}Ce and ^{137}Nd,[34] which have negative g factors[35] consistent with a $\nu s_{1/2} \otimes [\nu h_{11/2}]^2$ three-quasineutron configuration. The excitation energies of these isomers are independent of the proton number, as is the case for 5^- states in the corresponding core nuclei, also implying a neutron character for these states. For this γ-soft nucleus it would be relatively easy for the valence $h_{11/2}$ neutron to induce a significant negative γ deformation close to the collective $\gamma = -60°$ oblate shape. A similar structure has recently been proposed for the low-lying negative-parity states in ^{132}Ba.[11]

The two transitions of energies 632 and 928 keV, placed on top of the 11^- state at 4241 keV may form part of a band built on the $\nu s_{1/2} \otimes [\nu h_{11/2}]^3$ oblate four-quasineutron configuration. Alternatively, this band could be associated with the prolate decoupled band expected for the $\pi h_{11/2} \otimes \pi g_{7/2}$ configuration. Such sidebands built on the prolate $\pi h_{11/2} \otimes \pi g_{7/2}$ configuration have been predicted and observed[36,37] in the well-deformed light barium nuclei. Furthermore, rotational sidebands built on both of the proposed configurations, namely prolate-proton and oblate-neutron configurations, have been observed at similar excitation energies in ^{132}Ba.[11]

3. The $\Delta I = 1$ band: Systematics of collective oblate rotation

The existence of strongly coupled $\Delta I = 1$ rotational bands with distinct properties has been established for several nuclei of this mass region including odd-Z,[7–9] doubly-odd,[10] and even-even[11] nuclei. The characteristic features of these bands are: (1) Intense $\Delta I = 1$ transitions. Where the $E2$ crossovers have been observed, values of

$$B(M1;\Delta I = 1)/B(E2;\Delta I = 2) \sim 10(\mu_N/eb)^2$$

have been extracted; (2) no signature splitting, i.e., the $\Delta I = 1$ transition energies increase smoothly with spin; (3) negative $E2/M1$ mixing ratios $\delta_{E2/M1}$ for the $\Delta I = 1$ transitions, when measured; and (4) relatively low dynamic moments of inertia $\mathcal{J}^{(2)} = dI/d\omega$, typically only 60% of values for known prolate bands.

In the case of ^{131}La,[7] such a band was identified with the $\pi h_{11/2} \otimes [\nu h_{11/2}]^2$ configuration at a shape close to

the collectively rotating $\gamma=-60°$ oblate shape. Comparison with cranked shell-model (CSM) calculations indicated that it is the rotational alignment of upper midshell $h_{11/2}$ neutrons that induces the shape change towards the collective oblate shape, especially for the γ-soft nuclei of this mass region. However, the $\pi h_{11/2}[505]\frac{11}{2}^-$ orbital is strongly down sloping in energy on the oblate side ($\beta_2<0$) of a Nilsson diagram and may also contribute to the stability of the oblate shape. Indeed, collective oblate bands built on this single high-Ω $\pi h_{11/2}$ orbital have recently been observed[38] to low spin ($\frac{11}{2}^-$) in light iodine nuclei. For such an oblate shape, the $[505]\frac{11}{2}^-$ orbital is near to the proton Fermi surface for proton numbers $Z\sim 56$.

The strongly coupled nature of the $h_{11/2}$ proton produces several experimentally observable effects. First, the high Ω gives rise to a regular $\Delta I=1$ band with no signature splitting. Secondly, the large positive g factor of the $h_{11/2}$ proton leads to a sizeable component of the magnetic moment μ perpendicular to the spin I of the nucleus. In terms of the geometrical model of Dönau and Frauendorf,[39] the high-Ω orbital will induce a strong $B(M1)$ rate and will produce an $E2/M1$ mixing ratio $\delta_{E2/M1}$ for the $\Delta I=1$ transitions whose sign reduces to the sign of the quadrupole moment, i.e., $\mathrm{sgn}[\delta_{E2/M1}]=\mathrm{sgn}[Q_0]$. Hence, for an oblate shape with $Q_0<0$, then $\delta_{E2/M1}$ will be negative.

The intense $\Delta I=1$ band observed in ^{136}Ce and shown in Fig. 2 has no signature splitting. From the observed intensities of the $\Delta I=1$ transitions, together with upper limits for the unobserved crossover $E2$ transitions, a conservative lower limit for the $B(M1;\Delta I=1)/B(E2;\Delta I=2)$ ratios of 10 $(\mu_N/eb)^2$ is obtained for the band, consistent with values obtained in similar $\Delta I=1$ bands in ^{130,131}La.[10,7] The $E2/M1$ mixing ratio $\delta_{E2/M1}$ could only be extracted for two of the $\Delta I=1$ transitions in ^{136}Ce but was found to be negative thereby implying an oblate shape for the band. A relatively low dynamic moment of inertia

$$\mathcal{J}^{(2)}=dI/d\omega=4\hbar^2/\Delta E_\gamma<20\hbar^2\ \mathrm{MeV}^{-1}$$

was extracted for this band for rotational frequencies below $\hbar\omega=0.45$ MeV.

With regard to the discussed configurations for the negative- and positive-parity sidebands, an obvious choice for the configuration associated with the $\Delta I=1$ band in ^{136}Ce is the $\pi g_{7/2}\otimes\pi h_{11/2}\otimes[\nu h_{11/2}]^2$ two-quasiproton–two-quasineutron configuration at $\gamma\sim-60°$. This structure has recently been proposed for a similar $\Delta I=1$ band in ^{132}Ba;[11] this band was populated, however, with only $\sim 3\%$ of the intensity of the $2^+\rightarrow 0^+$ transition. Comparing the collective oblate bands systematically observed in this mass region, it is possible to write down quasiparticle configurations for these structures observed in odd-Z, doubly-odd, and even-even nuclei, i.e.,

^{131}La, ^{133,137}Pr: $\pi h_{11/2}\otimes[\nu h_{11/2}]^2$ (odd Z),

^{130}La: $\nu g_{7/2}\otimes\pi h_{11/2}\otimes[\nu h_{11/2}]^2$ (odd odd),

^{132}Ba, ^{136}Ce: $\pi g_{7/2}\otimes\pi h_{11/2}\otimes[\nu h_{11/2}]^2$ (even even).

The common element of these bands is a pair of rotationally aligned low-Ω $h_{11/2}$ neutrons coupled to the $[505]\frac{11}{2}^-$ high-Ω $h_{11/2}$ proton orbital. As previously stated, the aligned neutrons drive the γ-soft core to the collective oblate $\gamma\sim-60°$ shape where the $h_{11/2}$ proton is responsible for both the regular (no signature splitting) sequence of the $\Delta I=1$ transitions and for the large $B(M1)/B(E2)$ ratios. The extra positive-parity quasiparticles for doubly odd ^{130}La, and even-even ^{132}Ba and ^{136}Ce, showing relatively flat Routhians with respect to γ, are essentially spectators with no influence on the nuclear shape.

The dynamic moments of inertia for the oblate bands in ^{130,131}La, ^{132}Ba, and ^{136}Ce are compared in Fig. 4. These values are much lower ($\sim 60\%$) than those extracted for prolate rotational bands in neighboring nuclei and indicate a somewhat different shape and deformation. A classical ellipsoid rotating around an axis perpendicular to its symmetry axis (collective rotation) has a moment of inertia given by $\mathcal{J}=\mathcal{J}_0(1+0.31\beta_2)$, where $\mathcal{J}_0$ relates to a spherical shape. In this simple picture, an increase in prolate (oblate) deformation $\beta_2>0$ ($\beta_2<0$) results in an increase (decrease) in $\mathcal{J}$. A quantitative comparison is difficult to make, however, since the pairing-induced irrotational flow, which reduces $\mathcal{J}$ from its rigid value, is altered by the quasiparticle blocking of some of the pairing correlation strength. The preceding simple argument suggests, however, that the low dynamic moments of inertia observed for the oblate bands in this mass region imply an enhanced (more negative) quadrupole deformation. Moreover, cranked shell-model calculations performed as a function of the quadrupole deformation, for an oblate shape, indicate that the Routhians of the valence high-Ω $h_{11/2}$ proton orbitals fall sharply with increasing (negative) deformation towards $\beta_2=-0.2$, and then drop more gradually towards $\beta_2\sim-0.4$, which represents an oblate shape with a 2:3 axis ratio. Hence, such high-Ω $h_{11/2}$

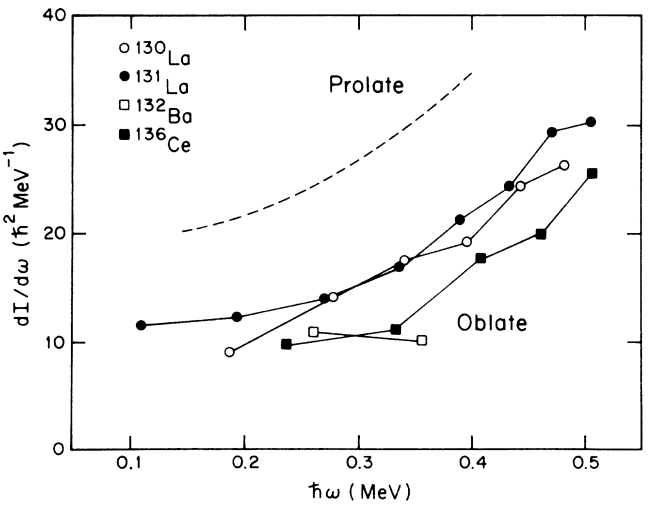

FIG. 4. A comparison of the dynamic moments of inertia ($dI/d\omega=4\hbar^2/\Delta E_\gamma$) for collective oblate bands in this mass region, including odd-Z (^{131}La), doubly odd (^{130}La), and even-even (^{132}Ba, ^{136}Ce) nuclei. The dashed line represents the moment of inertia expected for a prolate nucleus.

proton orbitals in an oblate nucleus introduce a β-driving force on the nuclear core to larger quadrupole deformation. In contrast, the valence low-Ω $h_{11/2}$ neutron orbitals are more flat with respect to the quadrupole deformation, favoring a shape closer to the spherical $\beta_2=0$ shape.

C. Other band structures in ^{136}Ce

Two sets of weak coincident transitions with intensities $<2\%$ of the $2^+\rightarrow 0^+$ transition were established from this analysis. One group of transitions appears to be of $\Delta I=1$ character, while the second group appears to be of $\Delta I=2$ character. However, because of the weakness of the transitions, it was not possible to experimentally determine the multipolarities of the transitions. Tentative interpretations of these weak structures are presented in the following.

1. The $\Delta I=1$ transitions

A set of transitions (not included in Fig. 2) of energies 189-158-201-169-384-234-293 keV was established, and because of the low energies of the transitions, they are assumed to be $\Delta I=1$ transitions. One possible explanation is that they form a collective oblate band ($\gamma\sim -60°$) similar to the one already seen in ^{136}Ce although the energy spacings are somewhat irregular. Furthermore, two such $\Delta I=1$ sequences have recently been established in the even-even ^{132}Ba nucleus.[11]

2. The $\Delta I=2$ transitions

A regular set of weak coincident transitions of energies 425-495-568-640-706 keV, as shown to the left in Fig. 2, appears to be in coincidence with the ground-state band of ^{136}Ce. The transitions are most likely of stretched quadrupole character because of the regular nature of these γ rays observed to high transition energies. This set of transitions has a fairly constant energy spacing $\Delta E_\gamma\sim 70$ keV which, assuming the quadrupole nature of these transitions, corresponds to a dynamic moment of inertia $\mathcal{J}^{(2)}\sim 57\hbar^2$ MeV^{-1} (cf. $\mathcal{J}^{(2)}<20\hbar^2$ MeV^{-1} for the oblate $\Delta I=1$ band, shown in Fig. 4) that is in excess of the spherical rigid-body estimate. Such a high moment of inertia is comparable to that observed in the highly deformed band of ^{132}Ce (Ref. 13) and is close to the rigid-body estimate for a 3:2 axis ratio. Hence it is speculated that these transitions may be part of the corresponding band in ^{136}Ce. If this is the case, the band exists at a much lower excitation energy in ^{136}Ce compared to ^{132}Ce with a relatively low band-head spin. Indeed, recent TRS calculations[14,15] predict the highly deformed $[\nu i_{13/2}]^2$ configuration to lie at a relatively low excitation energy in ^{136}Ce.

IV. CONCLUSIONS

The high-spin properties of ^{136}Ce have been investigated. The prominent structure observed at high spins is a strongly populated $\Delta I=1$ band that is believed to be associated with the collective oblate rotation ($\gamma\sim -60°$) of a structure built on the $\pi g_{7/2}\otimes\pi h_{11/2}\otimes[\nu h_{11/2}]^2$ configuration. The properties of this band are similar to other collective oblate bands that have systematically been observed in nuclei with $Z=56$–58 in this mass region. The shape change to oblate, via the γ plane, is driven by the rotational alignment of upper-midshell $h_{11/2}$ neutrons. For such an oblate shape, the $h_{11/2}$ proton orbitals near the Fermi surface are negative β driving, which may stabilize the oblate nuclear shape. In addition, a shell gap exists in the Nilsson single-particle systematics for the proton number $Z=56$ at an oblate deformation $\beta_2<-0.3$. These features should help to stabilize the collective oblate shape at large deformations near the 2:3 axis ratio.

In contrast to the $\Delta I=1$ band showing a low moment of inertia, a weak band showing an enhanced moment of inertia, in excess of the spherical rigid-body estimate, was observed in coincidence with the low-lying states of ^{136}Ce. This band possibly corresponds to the $[\nu i_{13/2}]^2$ configuration that is partly responsible for the highly deformed prolate band ($\beta_2\geq 0.35$) in ^{132}Ce with a 3:2 axis ratio. Because of the weakness of this band, it would be worthwhile to further investigate the high-spin structures of ^{136}Ce using the sensitivity of a large array.

ACKNOWLEDGMENTS

This work was in part supported by grants from the National Science Foundation and from the United Kingdom Science and Engineering Research Council. One of us (I.J.) acknowledges receipt of a SERC postgraduate studentship during the course of this work.

*Present address: Oliver Lodge Laboratory, University of Liverpool, P.O. Box 147, Liverpool L69 3BX, United Kingdom.

[1] I. Ragnarsson, A. Sobiczewski, R. K. Sheline, S. E. Larsson, and B. Nerlo-Pomorska, Nucl. Phys. **A233**, 329 (1974).

[2] Y. S. Chen, S. Frauendorf, and G. A. Leander, Phys. Rev. C **28**, 2437 (1983).

[3] B. D. Kern, R. L. Mlekodaj, G. A. Leander, M. O. Kortelahti, E. F. Zganjar, R. A. Braga, R. W. Fink, C. P. Perez, W. Nazarewicz, and P. B. Semmes, Phys. Rev. C **36**, 1514 (1987).

[4] G. A. Leander, S. Frauendorf, and F. R. May, in *Proceedings of the Conference on High Angular Momentum Properties of Nuclei, Oak Ridge, 1982,* edited by N. R. Johnson (Harwood Academic, New York, 1983), p. 281.

[5] S. Frauendorf and F. R. May, Phys. Lett. **125B**, 245 (1983).

[6] G. Andersson, S. E. Larsson, G. Leander, P. Möller, S. G. Nilsson, I. Ragnarsson, S. Åberg, R. Bengtsson, J. Dudek, B. Nerlo-Pomorska, K. Pomorski, and Z. Szymański, Nucl. Phys. **A268**, 205 (1976).

[7] E. S. Paul, C. W. Beausang, D. B. Fossan, R. Ma, W. F. Piel, Jr., N. Xu, L. Hildingsson, and G. A. Leander, Phys. Rev. Lett. **58**, 984 (1987).

[8] L. Hildingsson, C. W. Beausang, D. B. Fossan, and W. F. Piel, Jr., Phys. Rev. C **37**, 985 (1988).

[9]N. Xu, C. W. Beausang, R. Ma, E. S. Paul, W. F. Piel, Jr., D. B. Fossan, and L. Hildingsson, Phys. Rev. C **39**, 1799 (1989).
[10]M. J. Godfrey, Y. He, I. Jenkins, A. Kirwan, P. J. Nolan, D. J. Thornley, S. M. Mullins, R. Wadsworth, and R. A. Wyss, J. Phys. G **15**, 671 (1989).
[11]E. S. Paul, D. B. Fossan Y. Liang, R. Ma, and N. Xu, Phys. Rev. C **40**, 1255 (1989).
[12]Y.-X. Luo, J.-Q. Zhong, D. J. G. Love, A. Kirwan, P. J. Bishop, M. J. Godfrey, I. Jenkins, P. J. Nolan, S. M. Mullins, and R. Wadsworth, Z. Phys. **A329**, 125 (1988).
[13]A. J. Kirwan, G. C. Ball, P. J. Bishop, M. J. Godfrey, P. J. Nolan, D. J. Thornley, D. J. G. Love, and A. H. Nelson, Phys. Rev. Lett. **58**, 467 (1987).
[14]R. Wyss (private communication).
[15]R. Wyss, J. Nyberg, A. Johnson, R. Bengtsson, and W. Nazarewicz, Phys. Lett. B **215**, 211 (1988).
[16]R. Ma, E. S. Paul, C. W. Beausang, S. Shi, N. Xu, and D. B. Fossan, Phys. Rev. C **36**, 2322 (1987).
[17]A. Kirwan (private communication).
[18]J. Nyberg (private communication).
[19]D. Ward, R. M. Diamond, and F. S. Stephens, Nucl. Phys. **A117**, 309 (1969).
[20]W. Dehnhardt, S. J. Mills, M. Müller-Veggian, U. Neumann, D. Pelte, G. Poggi, B. Povh, and P. Taras, Nucl. Phys. **A225**, 1 (1974).
[21]M. Müller-Veggian, Y. Gono, R. M. Lieder, A. Neskakis, and C. Mayer-Böricke, Nucl. Phys. **A304**, 1 (1978).
[22]N. Yoshikawa, Nucl. Phys. **A243**, 143 (1975).
[23]E. Dafni, F. D. Davidovsky, A. Gelberg, M. Haas, E. Naim, and G. Schatz, in *Proceedings of the International Conference on Hyperfine Interactions, Groningen, 1983,* edited by L. Niesen, F. Pleiter, and H. de Waard [Hyperfine Interactions **15/16**, 101 (1983)].
[24]L. Hildingsson, C. W. Beausang, D. B. Fossan, W. F. Piel, Jr., A. P. Byrne, and G. D. Dracoulis, Nucl. Instrum. Methods A **252**, 91 (1986).
[26]G. Palameta and J. C. Waddington, Nucl. Instrum. Methods A **234**, 476 (1985).
[27]K. S. Krane, R. M. Steffen, and R. M. Wheeler, Nuclear Data Tables A **11**, 351 (1973).
[28]K. S. Krane, At. Data Nucl. Data Tables **16**, 384 (1975).
[29]M. A. J. Mariscotti, G. Scharff-Goldhaber, and B. Buck, Phys. Rev. **178**, 1864 (1969).
[30]E. S. Paul, C. W. Beausang, D. B. Fossan, R. Ma, W. F. Piel, Jr., P. K. Weng, and N. Xu, Phys. Rev. C **36**,153 (1987).
[31]E. S. Paul, S. Shi, C. W. Beausang, D. B. Fossan, R. Ma. W. F. Piel, Jr., N. Xu, and P. K. Weng, Phys. Rev. C **36**, 2380 (1987).
[32]W. Starzecki, G. De Angelis, B. Rubio, J. Styczen, K. Zuber, H. Güven, W. Urban, W. Gast, P. Kleinheinz, S. Lunardi, F. Soramel, A. Facco, C. Signorini, M. Morando, W. Meczynski, A. M. Stefanini, and G. Fortuna, Phys. Lett. B **200**, 419 (1988).
[33]R. Wyss, A. Johnson, J. Nyberg, R. Bengtsson, and W. Nazarewicz, Z. Phys. A **329**, 255 (1988).
[34]J. Gizon, A. Gizon, R. M. Maier, R. M. Diamond, and F. S. Stephens, Nucl. Phys. **A222**, 557 (1974).
[35]A. Zemel, C. Broude, E. Dafni, A. Gelberg, M. B. Goldberg, J. Gerber, G. J. Kumbartzki, and K.-H. Speidel, Z. Phys. A **304**, 269 (1982).
[36]C. Flaum, D. Cline, A. W. Sunyar, and O. C. Kistner, Phys. Rev. Lett. **33**, 973 (1974).
[37]C. Flaum, D. Cline, A. W. Sunyar, O. C. Kistner, Y. K. Lee, and J. S. Kim, Nucl. Phys. **A264**, 291 (1976).
[38]Y. Liang, R. Ma, E. S. Paul, N. Xu, D. B. Fossan, J. Y. Zhang, and F. Dönau, Phys. Rev. Lett. **64**, 29 (1990).
[39]F. Dönau and S. Frauendorf, in *Proceedings of the Conference on High Angular Momentum Properties of Nuclei, Oak Ridge, 1982,* edited by N. R. Johnson (Harwood Academic, New York, 1983), p. 143; F. Dönau, Nucl. Phys. **A471**, 469 (1987).